Small-angle neutron scattering studies of vortex lattice morphology in YNi_2B_2C

C. D. Dewhurst [a,1], S. J. Levett [a], D. M^{c}K. Paul [b]

[a] *Institut Laue Langevin, 6 rue Jules Horowitz, 38042 Grenoble, France*
[b] *Department of Physics, University of Warwick, Coventry CV4 7AL, UK*

Abstract

High-resolution small-angle neutron scattering studies of the vortex lattice (VL) in YNi_2B_2C allow us to separate Bragg scattered intensities from the multi-domain VL that exists for $B \parallel c$. The first-order 45° reorientation of the VL at a field H_1 is broadened by weak vortex pinning and characterised by a redistribution of domain populations between the low- and high-field vortex structures through the transition with no continuous distortion between the two phases. As nonlocal effects become weaker with increasing temperature, $H_1(T)$ *decreases* while the field at which the VL becomes square, $H_2(T)$, *increases*. The nature of the high-field rhombic VL ($H_1 < H < H_2$) close to $H_{c2}(T)$ is discussed.

Key words: Vortex Lattice, Small-Angle Neutron Scattering, YNi_2B_2C, Borocarbide

The lowest energy configuration for a repulsive array of magnetic-flux lines forming the vortex lattice (VL) is usually a two-dimensional (2D) hexagonal lattice, although the energy difference between hexagonal and square packing configurations is small ($\simeq 2$ %). In the tetragonal borocarbide materials [RE]Ni_2B_2C (RE = Lu,Y,Er,Tm,Ho,Dy) Fermi-surface anisotropy, combined with the relatively clean *s*-wave superconductivity results in significant nonlocal effects and a host of magnetic field, temperature and magnetic order dependent vortex lattice phases with either hexagonal, rhombic or square VL symmetry [1–3]. Meanwhile in the proposed *p*-wave and *d*-wave materials observation of a square VL provides strong evidence for these order parameter symmetries [4,5]. Several authors have been able to describe VL structures well below T_c using nonlocal corrections to the London model [6], or considering the effects of non *s*-wave order parameter symmetries [7]. Close to T_c a Ginzbug-Landau approach may be adopted coupling any Fermi surface or order parameter anisotropy via the addition of higher order terms in the GL expansion of the free energy [8].

SANS measurements were carried out using the D22 diffractometer, configured in a high-resolution mode, at the Institut Laue Langevin, Grenoble, France. The sample and electromagnet could be tilted together about a horizontal or vertical axis to satisfy the Bragg condition for any particular diffraction spot. Background measurements, taken with the sample in the normal state, have been subtracted from each pattern prior to analysis. The YNi_2B_2C crystal was grown with isotopic ^{11}B to reduce neutron absorption.

Figure 1(a) shows the diffraction image from the VL following field cooling in 100 mT to 4.5 K followed by a field-oscillation of 10 % the main field value (FCO). The FCO VL preparation technique effectively 'shakes' the VL from weak pinning sites in an attempt to achieve a vortex arrangement closer to equilibrium [3]. The positions of the twelve Bragg peaks do not lie on a circle of constant $|q|$ expected for a VL with hexagonal symmetry. Rather, four intense Bragg reflections and two weaker peaks on either side correspond to two domains of rhombic VL. By fitting 2D Gaussian func-

[1] Corresponding author E-mail: dewhurst@ill.fr

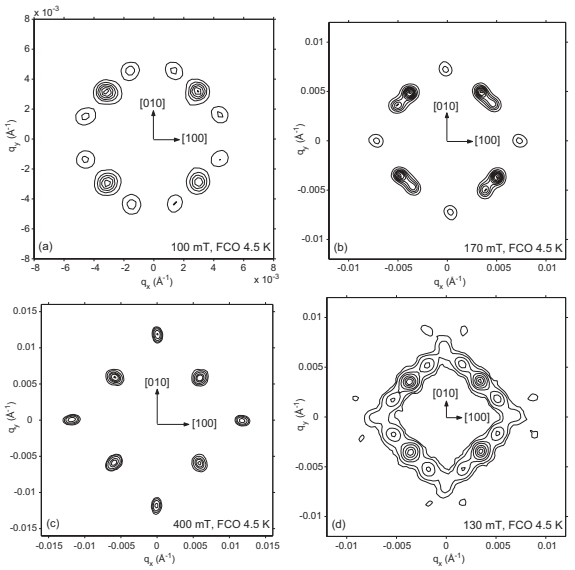

Fig. 1. SANS from the VL in YNi_2B_2C at 4.5 K for applied fields of (a) 100 mT, (b) 170 mT and (c) 400 mT. (d) Coexistence of low- and high-field VL phases at 130 mT.

tions to the multidetector data the VL opening angle, $\beta(\simeq 54^\circ)$, can be accurately determined. The integrated intensity of the weaker spots at a slightly larger $|q|$ differ from the four strong spots by around 9%, consistent with the expected $1/q^5$ reflectivity from the VL.

Figure 1(b) shows the VL at 170mT, above the field H_1, where the rhombic VL has reoriented by 45 ° and $\beta(\simeq 82^\circ)$ has abruptly switched to a value greater than 60°. Eight first-order Bragg peaks are present in pairs with each pair split azimuthally and the visible higher-order (1,1) reflections extended in the radial direction. With further increasing applied field β increases continuously until at a field H_2 $\beta = 90$ ° and single domain square vortex lattice is observed (Fig. 1(c)).

The coexistence of both low- and high-field rhombic VL phases around the reorientation transition, H_1, is shown in Figure 1(d) at 170 mT, 4.5 K, while Figure 2 shows β over a wide field range from the low- to high-field rhombic phases until the lattice becomes square. High resolution SANS has allowed us to determine β accurately through the coexistence region. The vortex lattice structure does not appear to deform smoothly through H_1 synonymous with a continuous reorientation transition. Instead, β takes well defined values corresponding to the VL phases above and below H_1. The inset to Figure 2 shows the scattered intensity associated with the low- and high field phases as a function of field through the coexistence regime, normalised by a q^5 and B^2 term to remove any q and field dependence of the reflected intensity from the VL. The broadened nature of the suggested first-order transition at H_1 is due to weak static disordering (pinning) of the VL. An

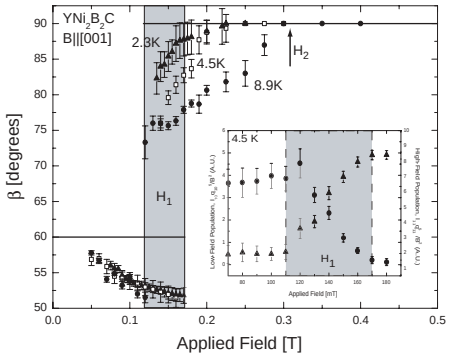

Fig. 2. Apex angle, β, vs. field. Inset: Relative populations of the coexisting low- and high-field phases (shaded region).

entirely analogous behaviour is seen in the nonuniform melting of the VL in the high-temperature superconducting $Bi_2Sr_2CaCu_2O_{8+\delta}$ [9] and consistent with general arguments pertaining to first-order transitions in the presence of weak disorder.

The nature of the temperature dependence of VL reorientation transitions at H_1 and H_2 is of ongoing study although general trends can be identified from the data presented in Figure 2. The first-order reorientation transition, $H_1(T)$, *decreases* while the continuous transition to a square VL at $H_2(T)$ *increases* with increasing temperature. Since nonlocal effects become weaker at higher temperatures (decreasing mean free path), Figure 2 suggests that the phase diagram is dominated by the high-field rhombic vortex phase ($H_1 < H < H_2$) at higher temperatures. A broadly similar behaviour is observed as a function of impurity doping in $LuNi_2B_2C$ [10]. Incorporation of higher order terms into the GL expansion for the free energy predicts that the vortex lattice should be rhombic close to $H_{c2}(T)$ for fields below H_2 [8]. H_2 itself is expected to intercept $H_{c2}(T)$ implying a square vortex lattice forms immediately upon high-field cooling ($H > H_2$) through $H_{c2}(T)$, in contrast to ref. [2] but in agreement with our ongoing high-resolution measurements.

References

[1] D. M^{c}K Paul et al., Phys. Rev. Lett. **80**, 1517 (1998).

[2] M. R. Eskildsen et al., Phys. Rev. Lett. **86**, 5148 (2001).

[3] S. J. Levett et al., Phys. Rev. B **65** (2002).

[4] T. M. Riseman et al., Nature **396**, 242 (1998).

[5] R. Gilardi et al., Phys. Rev. Lett. **88**, 217003 (2002).

[6] V. G. Kogan et al., Phys. Rev. B **55**, R8693 (1997).

[7] M. Franz et al., Phys. Rev. Lett. **79**, 1555 (1998).

[8] K. Park, D. A. Huse, Phys. Rev. B **58**, 9427 (1998).

[9] A. Soibel et al., Nature **406**, 282 (2000).

[10] P. L. Gammel et al., Phys. Rev. Lett. **82**, 4082 (1999).